Proceedings of the 6th International Conference on Recrystallization and Grain Growth (ReX&GG 2016) *Edited by: Elizabeth A. Holm, Susan Farjami, Priyadarshan Manohar, Gregory S. Rohrer, Anthony D. Rollett, David Srolovitz, and Hasso Weiland*
TMS (The Minerals, Metals & Materials Society), 2016

Recrystallization Behavior of δ-Ferrite in the Ti-Alloyed Low Density Steel

Xiangyu Xu[1], Xuemin Wang[1], Jianzhe Li[2], Jian Zhang[2]

[1]Collaborative Innovation Center of Steel Technology, University of Science and Technology Beijing; 30 Xueyuan Road, Haidian District; Beijing, 100083, P. R. China
[2]School of Materials Science and Engineering, University of Science and Technology Beijing; 30 Xueyuan Road, Haidian District; Beijing, 100083, P. R. China

Keywords: δ-ferrite, recrystallization, low density steel, Ti-alloyed steel

Abstract

δ-ferrite steel designed with high aluminum low carbon and manganese meets the requirements of plate steel for lightweight and corrosion-resistant. The toughness of the steel is low because of the ordering of Fe-Al and even some intermetallic compounds. Austenite phase region shrinked with the increase of aluminum content, therefore the δ-ferrite is stable from high temperature to room temperature. The phase transformation cannot be used to refine grain, while the recrystallization is the only way to refine grain. The annealing recrystallization of steels after hot deformation were studied. The static recrystallization behavior has been studied by Gleeble. The grain size of 0.014Ti steel after annealing reaches about 5 μm, and the full-thickness Charpy impact is 55 J. With the content of Ti increasing, precipitated TiC pinning grain boundaries and dissolved Ti atoms interacting with the grain boundaries, inhibit recrystallization. In the same deformation process, the grains of 0.044Ti steel are more prolate and coarse. After annealing at 750 ℃, the full-thickness Charpy impact is 38J.

Introduction

With the rapid development of marine engineering, the new demand on properties of plate steels for offshore structure was proposed, such as high strength, high toughness, corrosion resistance, good weldability and low weight. Currently, the research on low density steel are mainly for automobile sheet, by adding a lot of aluminum in steel [1-6]. It was found that while aluminum content up to 6 percent, the density would be reduced by 10 percent [6]. Also, Al bearing steels provide high corrosion resistance because of improving the protective capablility of the inner rust layer. Aluminum is ferrite forming elements, and the austenite phase area could be strongly reduced or even disappear, so γ-α transformation could not be used to refine grain. With the aluminum content increasing, there would be Fe-Al ordered structure and even intermetallic compound, which leads to grain boundary embrittlement and lower toughness. Grain refinement is usually used to improve the toughness, and recrystallization may be the simple and effective way to refine δ-ferrite grain size. C. Castan et al. reported dynamic recrystallization mechanisms of δ-ferrite [7].
Titanium carbonitride could prevent austenite grain growth, inhibit grain growth during recrystallization, and also contribute greatly to the strength by the precipitation strengthening effect [8, 9].

The study described here focuses on δ-ferrite recrystallization behavior and the effect of titanium content on the recrystallization behavior. The study points toward design of new low density offshore plate.

Experimental

The experimental materials are Ti-added high-aluminum low-carbon low-manganese steels, and the chemical compositions of the steels are listed in Table Ⅰ. Titanium content of 2# steel is higher than 1# steel. The experimental steels were melted in a high frequency induction furnace, cast as 25 kg ingots and forged into 80 mm thick billets at 1100 ℃. After that, the billets were heated to 1100 ℃ and held for 30 min, and then hot rolled. During hot rolling, the billet was subjected to 86% reduction to final thickness of 11 mm. Finally, the plates were water-quenched to room temperature.

The interrupted compression test was performed using a Gleeble-1500 thermo-simulator, the strain was 0.25. The impact tests of Charpy notch were carried out at -20 ℃. The thin foils were observed by Transmission Electron Microscopy (JEM 2100), and were prepared by twin-jet electropolished in a mixture of 5% perchloric acid and 95% ethyl alcohol at -45~-35 ℃ using voltage of 55-65 V. SEM was used to observe the fracture morphology.

Table Ⅰ. Chemical Composition of The Experimental Steels (wt %)

Steel	C	Al	Mn	Ti	Ni	Si	S
1#	0.044	4.20	1.15	0.014	0.78	0.33	0.0075
2#	0.047	4.08	0.75	0.044	0.96	0.26	0.0026

Results and Discussion

The phase property diagrams were calculated by Thermal-calc software, as shown in Figure 1. The maximum percentage of austenite content of both experimental steels are less than 5%, and the matrix microstructure of both experimental steels are δ-ferrite.

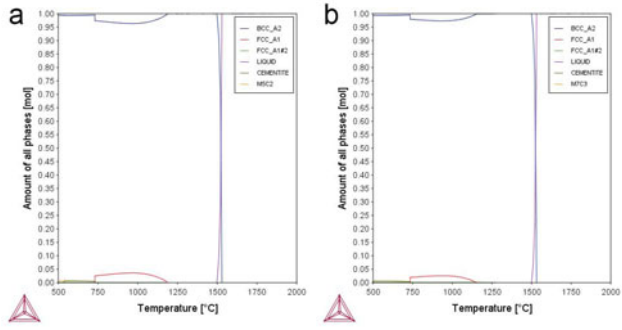

Figure 1. Phase property diagrams calculated by Thermal-calc software
(a) 1# steel, (b) 2# steel

The softening occurring during the holding interval between the first and second compression was expected to be mainly due to static recrystallization. The fractional softening (FS) was calculated by the offset-stress method [10-12], and the offset strain selected 0.002. Since recrystallization is usually assumed to begin at FS of 0.2. FS and the recrystallized fraction (FX) was evaluated by the following expressions:

$$FS = (\sigma_m - \sigma_2)/(\sigma_m - \sigma_1) \quad (1)$$

$$FX = (FS - 0.2)/(1 - 0.2) = (FS - 0.2)/0.8 \quad (2)$$

Where σ_m is the flow stress at the end of the first deformation, and σ_1 and σ_2 are the yield stresses. The calculation results of FS and FX are presented in Figure 2. The recrystallization stop temperature of both steels are below 750 ℃. In actual rolling practice the holding time during passes is 10-30s therefore the definition of recrystallization stop temperature is the temperature at which the recrystallization will not take place during the holding time. In contrast, FS and FX of 1# steel are higher than 2#, so with titanium content increasing, recrystallization temperature or non-recrystallization temperature would also improve.

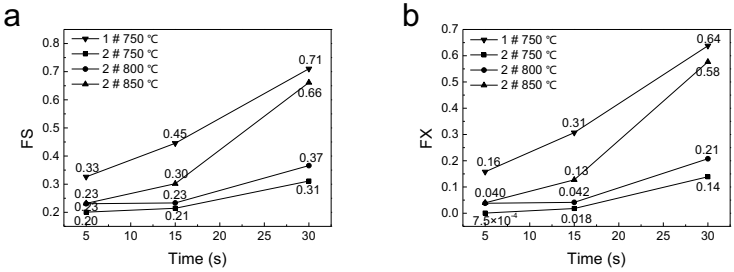

Figure 2. Calculation results of FS and FX

According to the result of interrupted compression test, the hot rolling process was designed, and the microstructure of cross section as-rolled is shown in Figure 3. During the rolling process, there may be two stages, incomplete recrystallization region and none recrystallization region respectively. The grain as-rolled was elongated, and the grain size of 2# steel is slightly more prolate and coarse than of 1# steel.

The as-rolled samples were annealed for 5 min and the microstructure is shown in Figure 4. It can been seen that after annealing at 800 ℃ and 830 ℃ for 1# steel, the elongated grain remained. However, after annealed at 850℃, and the grains become equi-axed with the grain size growing up to about 70 μm. Since the gain size of the sample as-rolled and annealed at 830 ℃ was too small to observe under OM, EBSD was applied to analyzing, as shown in Figure 5. After annealing, the density of small-angle grain boundary is reduced. Comparing with as-rolled samples, the grain became polygonal, but some grain were still in long strip. The grain size was about 5 μm.

The recrystallization behavior of 2# steel was similar to 1#. After annealing at 850 ℃, the recrystallization was completed, the grains become equi-axed, and the grain size was about 50 μm, which is slightly smaller than the 1# steel. The solid solution titanium has a drag effect, which inhibits recrystallization. In addition, titanium carbonitride precipitates have an effect on

pinning the grain boundaries, and inhibiting grain growth. Figure 6 shows the precipitates in the steel as-rolled and after annealed. The precipitates size of 2# steel was similar to 1#, but the density increased significantly. Therefore, with the titanium content increasing, the recrystallization temperature is elevated.

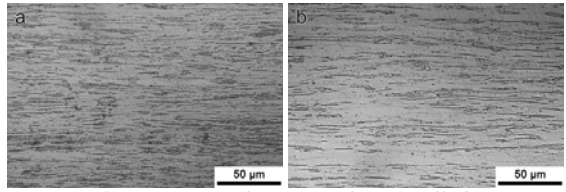

Figure 3. OM microstructure of cross section as-rolled (a) 1# steel, (b) 2# steel

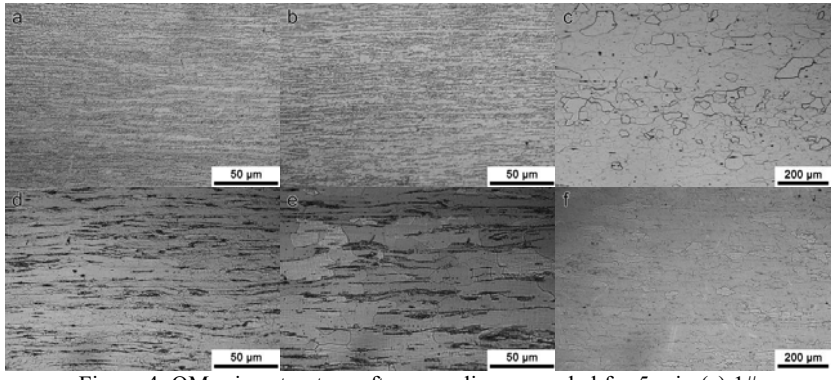

Figure 4. OM microstructure after annealing, annealed for 5 min (a) 1# steel annealed at 800 ℃, (b) 1# steel annealed at 830 ℃, (c) 1# steel annealed at 850 ℃, (d) 2# steel annealed at 750 ℃, (e) 2# steel annealed at 800 ℃, (f) 2# steel annealed at 850 ℃

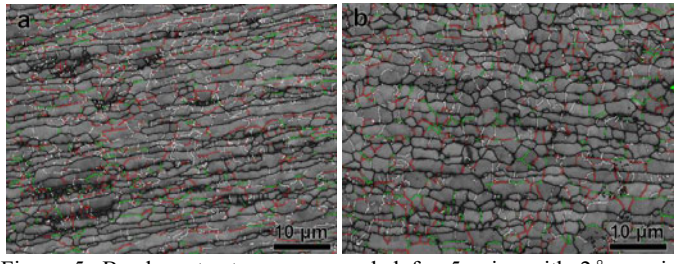

Figure 5. Band contrast maps, annealed for 5 min, with 2° grain boundaries in white, 5° in red, 10° in green, and 15° in black (a) as-rolled, (b) annealed at 830 ℃ for 5 min

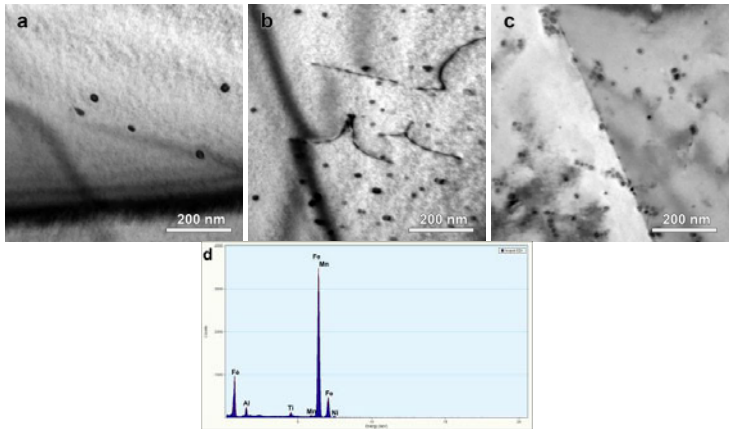

Figure 6. TEM images (a) 1# steel as-rolled, (b) 2# steel as-rolled, (c) 2# steel annealed at 850 ℃ for 5 min, (d) EDS spectrum of precipitate

The mechanical properties of the experimental steels are listed in Table Ⅱ. The steel showed low yield ratio and high elongation. The full-thickness Charpy impact reaches 55 J while the grain size is 5 μm. There is a significant negative correlation between the toughness and the grain size. Fig. 8 shows the fracture morphology of extending zone for 1# steel annealed at 830 ℃. Dimple fracture and quasi-cleavage fracture coexist. Due to the low metallurgical level for vacuum induction furnace, there is a large number of MnS inclusions in the steel, as shown in Figure 7, and the size of the inclusions reaches micron level, which would extremely reduce the toughness.

Table Ⅱ. Mechanical Properties of the Experimental Steels

	Rp0.2 (MPa)	Rm (MPa)	A (%)	-20 ℃ Akv (J)
1# steel as-rolled	660	715	18.8	53
2# steel as-rolled	539	738	20.4	38
1# steel annealed at 830 ℃	440	702	23.2	55
2# steel annealed at 750 ℃	556	626	27.3	36
2# steel annealed at 850 ℃	353	639	23.2	24

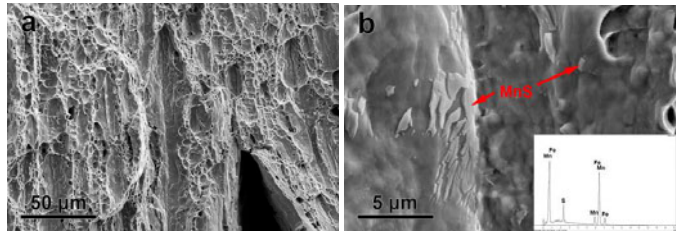

Figure 7. SEM images of the fracture morphology of extending zone for 1# steel annealed at 830 ℃ for 5 min

Conclusion

The matrix microstructure of the experimental steels are δ-ferrite, owing to the Ti-added high-aluminum low-carbon low-manganese alloy design. The non-recrystallization of both steels are below 750 ℃. In the same rolling process, the grain of 2# steel are more prolate and coarse. The drag effect from the solid solution titanium and titanium carbonitride precipitates pinning the grain boundaries, lead to recrystallization temperature increasing and inhibiting grain growth. By appropriate rolling-annealing process, the excellent mechanical property is obtained. The grain size of 1# steel after annealing at 830℃ for 5 min reaches about 5 μm, and the full-thickness -20 ℃ Charpy impact is 55 J. Impact fracture is dimple fracture and quasi-cleavage fracture in coexistence. Aggregation state of MnS inclusions extremely reduces the toughness.

References

1. H. Kim, D.-W. Suh and N. J. Kim, "Fe–Al–Mn–C lightweight structural alloys: a review on the microstructures and mechanical properties," *Science and Technology of Advanced Materials*, 14 (2013), 014205.
2. F. Yang et al., "Tensile deformation of low density duplex Fe–Mn–Al–C steel," *Materials & Design*, 76 (2015), 32-39.
3. C. Zhao et al., "Effect of annealing temperature on the microstructure and tensile properties of Fe–10Mn–10Al–0.7C low-density steel," *Materials & Design*, 91 (2016), 348-360.
4. L. Zhang et al., "Work hardening behavior involving the substructural evolution of an austenite–ferrite Fe–Mn–Al–C steel," *Materials Science and Engineering: A*, 640 (2015), 225-234.
5. R. Rana, C. Lahaye and R. K. Ray, "Overview of Lightweight Ferrous Materials: Strategies and Promises," *JOM*, 66 (2014), 1734-1746.
6. S. Y. Han et al., "Effects of Annealing Temperature on Microstructure and Tensile Properties in Ferritic Lightweight Steels," *Metallurgical and Materials Transactions A*, 43 (2011), 843-853.
7. C. Castan, F. Montheillet and A. Perlade, "Dynamic recrystallization mechanisms of an Fe–8% Al low density steel under hot rolling conditions," *Scripta Materialia*, 68 (2013), 360-364.
8. M. Akben et al., "Dynamic precipitation and solute hardening in a titanium microalloyed steel containing three levels of manganese," *Acta Metallurgica*, 32 (1984), 591-601.
9. M. Arribas, B. López and J. M. Rodriguez-Ibabe, "Additional grain refinement in recrystallization controlled rolling of Ti-microalloyed steels processed by near-net-shape casting technology," *Materials Science and Engineering: A*, 485 (2008), 383-394.
10. Z. Wang et al., "Strain-induced precipitation in a Ti micro-alloyed HSLA steel," *Materials Science and Engineering: A*, vol. 529, pp. 459-467, 2011.
11. W. Sun and E. Hawbolt, "Comparison between static and metadynamic recrystallization-an application to the hot rolling of steels," *ISIJ international*, 37 (1997), 1000-1009.
12. K. Rao, Y. Prasad and E. B. Hawbolt, "Study of fractional softening in multi-stage hot deformation," *Journal of Materials Processing Technology*, 77 (1998), 166-174.